

1 **Environmental correlates of peatland carbon fluxes in a**  
2 **thawing landscape: do transitional thaw stages matter?**

3 **A. Malhotra and N. T. Roulet**

4 Department of Geography, McGill University, Montreal, Quebec, Canada

5 Correspondence to: A. Malhotra ([avni.malhotra@mail.mcgill.ca](mailto:avni.malhotra@mail.mcgill.ca))

6

7

8

9

10

11

12

13

14

15

16

17

18

19

20

21

22 **Abstract**

23 Peatlands in discontinuous permafrost regions occur as a mosaic of wetland types, each with  
24 variable sensitivity to climate change. Permafrost thaw further increases the spatial heterogeneity  
25 in ecosystem structure and function in peatlands. Carbon (C) fluxes are well characterized in  
26 end-member thaw stages such as fully intact or fully thawed permafrost but remain  
27 unconstrained for transitional stages that cover a significant area of thawing peatlands.  
28 Furthermore, changes in the environmental correlates of C fluxes, due to thaw are not well  
29 described: a requirement for modeling future changes to C storage of permafrost peatlands. We  
30 investigated C fluxes and their correlates in end-member and a number of transitional thaw  
31 stages in a sub-arctic peatland. Across peatland lumped CH<sub>4</sub> and CO<sub>2</sub> flux data had significant  
32 correlations with expected correlates such as water table depth, thaw depth, temperature,  
33 photosynthetically active radiation and vascular green area. Within individual thaw states,  
34 bivariate correlations as well as multiple regressions between C flux and environmental factors  
35 changed variably with increasing thaw. The variability in directions and magnitudes of correlates  
36 reflects the range of structural conditions that could be present along a thaw gradient. These  
37 structural changes correspond to changes in C flux controls, such as temperature and moisture,  
38 and their interactions. Temperature sensitivity of CH<sub>4</sub> increased with increasing thaw in bivariate  
39 analyses, but lack of this trend in multiple regression analyses suggested confounding effects of  
40 substrate or water limitation on the apparent temperature sensitivity. Our results emphasize the  
41 importance of incorporating transitional stages of thaw in landscape level C budgets and  
42 highlight that end-member or adjacent thaw stages do not adequately describe the variability in  
43 structure-function relationships present along a thaw gradient.

44  
45  
46  
47  
48  
49  
50

## 51 **1 Introduction**

52 Northern permafrost regions contain approximately 50% (1672 Pg) of the world's soil carbon  
53 (C) pool and peatlands store 277 Pg of this C (Schuur et al., 2008; Tarnocai et al., 2009).

54 Thawing permafrost is projected to act as a positive feedback to climate change via the release of  
55 soil C to the atmosphere and the magnitude of this feedback remains uncertain (Schuur et al.,  
56 2013). Peatlands in the permafrost regions are currently experiencing increased rates of thaw and  
57 related changes to abiotic and biotic components (structure) and elemental cycling (function;  
58 Camill, 2005; Osterkamp, 2005). Thawing peatlands are a mosaic of different wetland types,  
59 ranging from permanently frozen (*e.g.* *palsa*) to permafrost-free and minerotrophic fens (Luoto et  
60 al., 2004). Each component of these heterogeneous landscapes has distinct C function,  
61 contributing to uncertainties in estimating landscape level C budgets. Constraining the spatial  
62 variability in peatland C fluxes and related abiotic and biotic factors, is an essential step toward  
63 estimating the positive feedback potential of thawing permafrost on climate change.

64 Permafrost thaw in peatlands is associated with marked changes in ecosystem structure and  
65 function. Initial ground subsidence from thaw results in wet habitats due to a high water table  
66 (Smith et al., 2012). Relative to dry areas, the seasonal frost table thaws faster in wet areas,  
67 further increasing lateral flow of water to wet areas (Quinton et al., 2009). The increase in water  
68 table depth (WTD) leads to a vegetation shift toward wetter communities and an increase in  
69 graminoid species (Camill, 1999; Camill et al., 2001; Malmer et al., 2005). Rapid changes also  
70 occur in the microbial community, notably an increased activity of methane (CH<sub>4</sub>) and nitrogen  
71 cycling (Mackelprang et al., 2011). Associated with structural shifts, several functional changes  
72 have been observed in thawed permafrost peatlands. Typically plant productivity increases  
73 (Vogel et al., 2009), but so does autotrophic and heterotrophic respiration (Hicks Pries et al.,  
74 2013). Organic matter decomposition may decrease due to increased anoxic conditions after  
75 ground subsidence (Camill et al., 2001). Thus, there could be an initial increase in organic matter  
76 accumulation as a result of permafrost thaw (Turetsky et al., 2007; Vitt et al., 2000).  
77 Subsequently, decomposition may increase due to the increase in easily decomposable litter from  
78 community shifts toward more vascular plants (Hodgkins et al., 2014; Turetsky, 2004) and  
79 quantity of litter (Malmer et al., 2005). Regardless of the initial increase in C accumulation, the  
80 net radiative forcing of a recently thawed area is offset by an increase in CH<sub>4</sub> emissions  
81 (Johansson et al., 2006; Sitch et al., 2007; Turetsky et al., 2007). This increase in CH<sub>4</sub> emissions

82 may be a direct result of increased temperature on microbial processes or indirect consequences  
83 such as increases in plant mediated transport of CH<sub>4</sub> by increased graminoid abundance and  
84 increased anaerobic decomposition due to a high water table (Christensen et al., 2004). In  
85 addition to magnitude, the dominant pathway of methane production is also altered after thaw,  
86 shifting from CO<sub>2</sub> reduction (hydrogenotrophic) to acetate cleavage (acetoclastic; Hodgkins et  
87 al., 2014; McCalley et al., 2014). The change in pathway is likely related to shifts in vegetation,  
88 for example, a decrease in *Sphagnum* abundance could lead to an increase in pH and related  
89 increase in acetoclastic methanogens (Hines et al., 2008; Ye et al., 2012). Dissolved organic  
90 matter (DOM) is also more labile in the more thawed stages and there is increased export of  
91 DOM out of the peatland catchment (Hodgkins et al., 2014; Olefeldt and Roulet, 2012, 2014).  
92 Recent studies highlight the interactive controls on C fluxes, emphasizing that net radiative  
93 forcing of a thawing ecosystem depends on non-linear interactions among temperature, degree of  
94 anoxia and organic matter chemistry (Lee et al., 2012; Treat et al., 2014). For example, while  
95 temperature sensitivity of CH<sub>4</sub> flux increases in wet habitats (Olefeldt et al., 2013), ecosystem  
96 respiration is more sensitive in dry conditions (McConnell et al., 2013). Interactive controls on C  
97 fluxes are further complicated by the variable structural conditions as thaw progresses, and the  
98 overall effect on landscape level fluxes remains unconstrained.

99 Changes to peatland structure and function due to permafrost degradation have been studied  
100 using a chronosequence approach with sites that have intact permafrost, completely thawed  
101 permafrost and one or two intermediate stages (e.g., Bäckstrand et al., 2010; Turetsky et al.,  
102 2007; Vogel et al., 2009). While end-member and major thaw stages of the permafrost gradient  
103 have been well characterized for plant community structure and carbon cycling, the same is not  
104 true for the transitional vegetation communities. Carbon cycling in thawing permafrost regions is  
105 spatially heterogeneous (e.g. Belshe et al., 2012; Morrissey and Livingston, 1992; Zhang et al.,  
106 2012) and a significant portion of the landscape is in varying stages of thaw. Spatial  
107 heterogeneity and transitional stages are therefore important to the ecosystem level C exchanges.  
108 It is unclear whether 3 to 5 thaw classes of intact, intermediate and fully thawed permafrost can  
109 be used to adequately extrapolate landscape scale C fluxes and their abiotic and biotic correlates.  
110 Additional thaw stages may help resolve landscape scale C fluxes in models.

111 Our study aims to identify the abiotic and biotic factors (hereafter, correlates) that relate to C  
112 function and investigate how these correlates change along end-member and transitional  
113 permafrost thaw stages. Our research questions are: 1) which correlates best explain the CH<sub>4</sub> and  
114 CO<sub>2</sub> fluxes across all thaw stages at a peatland where permafrost is thawing? 2) How does the  
115 importance of these correlates change along a gradient of increasing thaw? Our selection of  
116 measured correlates was based on current understanding of C flux relationships with  
117 temperature, moisture, pH, nutrients and plant biomass. Given the interactive nature of controls  
118 on C fluxes and variable structural changes after thaw, we expected to see no relationship  
119 between dominant correlates of C flux and degree of thaw.

## 120 **2 Methods**

121

### 122 **2.1 Study site**

123 The study site, Stordalen mire is located 10 km east of Abisko in Sweden (68°22' N, 19°03' E).  
124 The Stordalen peatland complex consists of several landscape units and wetland types.  
125 Permafrost is present in the dry hummocky sections of the peatland (palsa mire). Also present are  
126 areas where permafrost is thawing or has disappeared with vegetation communities that have  
127 been classified as semi-wet, wet, and tall graminoid (Johansson et al., 2006; Kvillner and  
128 Sonesson, 1980). Generally, the drier areas of the peatland complex are composed of species  
129 such as *Empetrum hermaphroditum*, *Betula nana*, *Rubus chamaemorus*, *Eriophorum vaginatum*,  
130 *Dicranum elongatum* and *Sphagnum fuscum*. The wetter areas consist of species such as *E.*  
131 *vaginatum*, *Carex rotundata*, *S. balticum*, *E. angustifolium*, *C. rostrata*, *S. lindbergii*, and *S.*  
132 *Riparium*. The long term (1912-2003) mean precipitation measured at the Abisko Scientific  
133 Research Station (10 km from the site) is 303.3 mm, of which 150 mm occurs between June and  
134 September. The long term (1912-2009) mean annual temperature at the site is -0.5°C but has  
135 surpassed 0°C in the recent decades (summarized in Olefeldt and Roulet (2012) from  
136 observations made at Abisko Scientific Research Station). Smoothed mean annual temperature  
137 trends suggest a 2.5°C increase between 1913 and 2006. (Callaghan et al., 2010).

## 138 **2.2 Vegetation community and thaw stage selection**

139 Ten vegetation communities were selected across Stordalen to represent major stages along the  
140 thaw gradient. Selection of communities was based on an across site survey of dominant  
141 vegetation communities, coupled with characterization of water table depth and active layer  
142 thickness. The sequence of the 10 thaw stages was based on a survey of spring thaw depth and  
143 previously established vegetation community relationships with permafrost thaw (Johansson et  
144 al., 2006; Kvillner and Sonesson, 1980).

## 145 **2.3 Gas flux measurements**

146 Within each of the 10 selected communities 3 collars of 0.05 m<sup>2</sup> area each were inserted in the  
147 peat surface and served as a seal for the manual gas flux measurements; with the exception of 2  
148 communities that had only 2 collars each as they represent a small area in the mire (Table 1).  
149 Each community also had a PVC dip well installed to measure the water table depth.

150 Methane flux was measured using opaque chambers of volume 9 or 18 liters. Five headspace  
151 gas samples of 20 ml each were collected every 5 min over 20 min. Prior to collecting each  
152 sample, the headspace was mixed using a syringe. The collected headspace samples were  
153 analyzed within 24 hours for concentrations of CH<sub>4</sub> using a Shimadzu GC-2014 gas  
154 chromatograph with a flame ionization detector, after separation on a HayeSep-Q packed column  
155 at the Abisko Scientific Research Station. Helium was used as a carrier gas at the flow rate of 30  
156 ml min<sup>-1</sup>. Injector, column and detector temperatures were 120, 40 and 120 °C, respectively. A  
157 10-repetition run of known CH<sub>4</sub> standard (2 ppm concentration) was used to calibrate the GC  
158 before and after each sample run. Accuracy of the analysis (calculated with the standard  
159 deviation of the 10 standard replicates) was ±0.1 to 0.75%. Flux rates were then calculated using  
160 the slope of the linear relationship between gas concentrations and time. Only the relationships  
161 with a significant (p<0.05) R<sup>2</sup> above 0.85 for the 5 time points were kept to calculate fluxes. If  
162 one of the five samples deviated from the linear fit, flux was calculated without it as long as the  
163 R<sup>2</sup> was greater than 0.95. Methane was measured on 7 days and 12 days in the 2012 and 2013  
164 growing seasons, respectively.

165 For carbon dioxide flux measurements on the 28 collars, we used clear cylindrical polycarbonate  
166 chambers (13 liter volume). The air enclosed within the chambers was mixed by fans and

167 circulated through an infrared gas analyzer (PP Systems, Model EGM-4) that measured changes  
168 in CO<sub>2</sub> over 3-min measurement intervals (recording every 10 seconds for the first minute, and  
169 then every 30 seconds for the last 2 minutes). Over the 3 minute measurement period, on  
170 average, temperature in the chamber only increased by 1.9 °C. Measurements were performed  
171 for full sun, with a mesh cover and finally with a black shroud, so that data from varying light  
172 intensities could be collected. Photosynthetically active radiation (PAR) was measured (Model  
173 LI-190SA, LI-COR<sup>®</sup>, NE, USA) within each chamber over the sample interval. Fluxes were  
174 calculated using a linear regression of CO<sub>2</sub> concentration change over time. CO<sub>2</sub> was sampled on  
175 10 days during the 2013 growing season.

#### 176 **2.4 Ancillary measurements**

177 Each flux measurement of CO<sub>2</sub> or CH<sub>4</sub> was coupled with simultaneous measurements of soil  
178 temperature at 10 cm, air temperature, thaw depth and water table depth (WTD). Once during the  
179 2012 growing season, elevation (above sea level) of each collar was measured using a RTK-  
180 GPS.

181 Vegetation composition for vascular plants was surveyed once every growing season in each of  
182 the collars recording the percent cover of each species. In 2013, vascular green area (VGA) was  
183 also measured on 4 days during the growing season using species specific formulae based on  
184 leaf-geometry (Lai, 2012; Wilson et al., 2006). For each collar, the total number of green leaves  
185 per species was recorded along with width and length of 10 leaves for each species. The  
186 seasonality of VGA was modeled using a Gaussian fit and combined with a quadratic fit with  
187 elevation to extrapolate a spatially and temporally higher resolution dataset for VGA.

188 Throughout the manuscript we only use the modeled VGA.

189 Surface water was sampled near the collars on each CH<sub>4</sub> sampling day in thaw stages that had  
190 persistent water table throughout the growing season (Thaw stages 5, 7, 8, 9 and 10). Surface  
191 water samples were analyzed for pH and conductivity (Oakton<sup>®</sup> portable pH conductivity meter)  
192 and reduced conductivity was calculated by removing H ion concentrations from the  
193 conductivity. Subsequently, samples were filtered using Whatman<sup>®</sup> Glass Fiber Filters (0.45 μm  
194 pore size) and analyzed for dissolved organic carbon and total nitrogen using a Shimadzu TOC-  
195 V series Analyzer.

196 **2.5 Data analysis**

197 *CH<sub>4</sub> flux*- Each flux measurement was log<sub>10</sub> transformed after adding 12 mg CH<sub>4</sub> m<sup>-2</sup> d<sup>-1</sup> to the  
198 original value (to account for all the negative fluxes). Log<sub>10</sub> transformation decreased the skew in  
199 the raw data and improved the linear relationship between methane and other variables, allowing  
200 for the use of multiple linear regressions. Bivariate relationships with abiotic and biotic factors  
201 were explored with Spearman's rank-order correlations. To explore the relationship between  
202 environmental correlates and CH<sub>4</sub> flux, we used stepwise multiple linear regression. We used  
203 both additive and interactive effects to explore a best fit model, but found that interactive effects  
204 were either insignificant or had a weak contribution to the overall model. For ease of  
205 interpretation, given that our variables are already proxies for several interacting controls on  
206 methane fluxes, we only included additive effects in our final model. The best fit model met the  
207 necessary assumptions of normality and homoscedasticity of model residuals. Multicollinearity  
208 was checked using variance inflation factors (VIF), wherein any explanatory variable with VIF  
209 greater than 2 was removed from the model.

210 Arrhenius plots were utilized to study the temperature sensitivity of CH<sub>4</sub> flux, regressing the log  
211 of CH<sub>4</sub> flux with inverse of temperature in Kelvin.

212 *CO<sub>2</sub> flux*- We combined all CO<sub>2</sub> flux data using nonlinear regression of a rectangular hyperbola  
213 to describe the relationship of NEE and PAR (Bubier et al., 2003)-

214 
$$NEE = \frac{GP_{MAX} \times PAR \times \alpha}{PAR \times \alpha + GP_{MAX}} + A \quad (1)$$

215

216 Where the parameters are:

217 GP<sub>MAX</sub> - the maximum gross photosynthetic CO<sub>2</sub> capture at maximum PAR (μmol CO<sub>2</sub> m<sup>-2</sup> s<sup>-1</sup>)

218 α - the photosynthetic quantum efficiency (μmol CO<sub>2</sub> m<sup>-2</sup> s<sup>-1</sup> per μmol PAR m<sup>-2</sup> s<sup>-1</sup>)

219 A - the dark respiration at 0 °C (μmol CO<sub>2</sub> m<sup>-2</sup> s<sup>-1</sup>)

220 Other than PAR, we expected to see non-linear relationships between CO<sub>2</sub> flux and WTD, thaw  
221 depth, soil temperature and VGA, but we did not find significant relationships. Instead we found

222 linear relationships to be significant. Since our data were non-parametric, we used Spearman's  
223 correlation coefficients to quantify the link between CO<sub>2</sub> flux with abiotic and biotic variables.

224 *Thaw gradient analyses*- above analyses for CH<sub>4</sub> and CO<sub>2</sub> were repeated independently for each  
225 of the 10 thaw stages. Subsequently, strength (adjusted R<sup>2</sup> or Spearman's ρ) and direction of  
226 relationships between correlates and function variables were organized by thaw stage to observe  
227 whether there is a significant trend in changing correlates of CH<sub>4</sub> and CO<sub>2</sub> fluxes along the thaw  
228 gradient. The sequence of thaw stages along the gradient was based on a survey of spring thaw  
229 depth, as discussed in section 2.2. Multiple regressions were also performed for each thaw stage  
230 since CH<sub>4</sub> and CO<sub>2</sub> fluxes are not typically estimated using bivariate models. While the bivariate  
231 correlations identified how the dominant correlates change across the thaw gradient, multiple  
232 regressions across the thaw gradient provide a better idea of the changing interactive effects of  
233 abiotic and biotic correlates on CH<sub>4</sub> or CO<sub>2</sub> fluxes.

234 Lastly, we evaluated the relationship between CH<sub>4</sub> and CO<sub>2</sub> fluxes using a simple CH<sub>4</sub>: CO<sub>2</sub> flux  
235 ratio. To use a standardized measure of CO<sub>2</sub> flux we use the GP<sub>MAX</sub> from each thaw stage.

## 236 **3 Results**

### 237 **3.1 Across peatland C fluxes and correlates**

238 Mean and standard error of CH<sub>4</sub> flux across all collars from 2 years of sampling was 91.25±8.17  
239 mg CH<sub>4</sub> m<sup>-2</sup> d<sup>-1</sup>, ranging from -1.1±0.3 to 370.2±52.1 mg CH<sub>4</sub> m<sup>-2</sup> d<sup>-1</sup> (Table 1).

240 Strongest bivariate relationships between CH<sub>4</sub> flux and abiotic variables were with elevation,  
241 water table depth, pH, VGA, thaw depth and surface water C:N (Fig. 1). Significant but weaker  
242 relationships were also found with soil temperature and Julian day. TC, TN, conductivity and  
243 reduced conductivity did not have a significant relationship with CH<sub>4</sub> flux.

244 The best fit multiple regression model for CH<sub>4</sub> fluxes across the peatland included elevation,  
245 thaw depth, VGA and soil temperature, in decreasing order of contribution to the overall model,  
246 and these variables were able to explain 73% of the variance in CH<sub>4</sub> flux (Table 2). An  
247 alternative model that excluded elevation wherein the adjusted R<sup>2</sup> drops to 0.62, is also reported  
248 as it better isolated the effects of VGA, soil temperature and thaw depth. The contribution (beta

249 weights reported in brackets) of soil temperature (0.16) and thaw depth (-0.27) are similar in the  
250 model with or without elevation. The contribution of VGA increases from 0.26 to 0.58 when  
251 elevation is removed from the model.

252 Photosynthetically active radiation showed the strongest relationship with CO<sub>2</sub> fluxes, explaining  
253 55% of the variance observed in the flux data (Fig. 2). The rectangular hyperbola fit of NEE  
254 against PAR, Eq. (1), provided the following parameter estimates and standard errors for the  
255 across site lumped data: GP<sub>MAX</sub> was 4.24±0.26 μmol CO<sub>2</sub> m<sup>-2</sup> s<sup>-1</sup>, α was 0.027±0.005 μmol CO<sub>2</sub>  
256 m<sup>-2</sup> s<sup>-1</sup> per μmol PAR m<sup>-2</sup> s<sup>-1</sup> and A was -1.78±0.09 μmol CO<sub>2</sub> m<sup>-2</sup> s<sup>-1</sup>.

257 Water table depth and thaw depth showed weak relationships with NEE and GPP (calculated  
258 using NEE minus R<sub>eco</sub>; Table 3). Soil temperature was also related to R<sub>eco</sub> and NEE. NEE and  
259 R<sub>eco</sub> were most strongly related to the mean growing season VGA (Table 3).

### 260 **3.2 Correlate-function relationships within the thaw stages**

261 Along the thaw gradient, the strength and direction of bivariate relationships among  
262 environmental variables and CH<sub>4</sub> flux changed variably (Fig. 3). No significant trend along the  
263 thaw gradient was observed for the relationship between CH<sub>4</sub> flux and elevation, VGA (vascular  
264 green area) and WTD. Significant trends were observed with the water chemistry variables of  
265 pH, C:N, TC, TN and conductivity and strength of correlations between correlate and CH<sub>4</sub> flux  
266 increased as the permafrost thawed. However, these data were only available for thaw stages  
267 with a water table (thaw stages 5 to 10). Soil temperature, thaw depth and Julian day, with data  
268 available for each of the 10 thaw stages, showed significant trends along the thaw gradient in  
269 their correlation with the CH<sub>4</sub> flux (Fig. 4 a, b, and c). There was an increase in the amount of  
270 variance explained in the CH<sub>4</sub> flux by temperature as well as the slope of this relationship (Fig.  
271 5).

272 The parameter estimates from the best fit model of across peatland lumped flux data, as shown in  
273 Table 2, were used as inputs for individual multiple regression models for each thaw stage. The  
274 interactive effects of elevation, soil temperature, thaw depth and vascular green area (VGA)  
275 showed varying results across the thaw gradient (Fig. 6). The model R<sup>2</sup> values ranged from 0.09  
276 (insignificant) to 0.79 (significant with p<0.0001). Generally, elevation, soil temperature, thaw  
277 depth and VGA were better predictors of variance in CH<sub>4</sub> fluxes in the later stages of thaw.

278 Model fit was non-significant for stages 2 and 3, and therefore their slope coefficients are not  
279 reported in Fig 6.

280 The relationship of NEE with temperature and with PAR varied across the thaw gradient without  
281 a statistically significant trend. Generally there is a trend of increasing,  $GP_{MAX}$ ,  $\alpha$  and A, going  
282 from less thawed to more thawed stages (Table 4). Furthermore, the amount of variance of NEE  
283 explained by PAR was typically higher in the more thawed stages.

### 284 **3.3 The relationship between NEE and CH<sub>4</sub>**

285  $GP_{MAX}$  and CH<sub>4</sub> were positively correlated ( $\rho=0.56$ ,  $p=0.0021$ ; Fig. 7). We found that the best  
286 explanatory variables for CH<sub>4</sub>:  $GP_{MAX}$  ratio were *Sphagnum* percent cover ( $\rho = -0.72$ ,  $p=0.008$ ;  
287 and graminoid VGA ( $\rho = 0.63$ ,  $p=0.0004$ ). While graminoid VGA did not have any interactive  
288 effects with abiotic variables in explaining CH<sub>4</sub>:  $GP_{MAX}$  ratio, *Sphagnum* cover and soil  
289 temperature had a significant interactive effect (Table 5)

## 290 **4 Discussion**

291 We identified the major abiotic and biotic correlates of the ecosystem – atmospheric exchanges  
292 of CO<sub>2</sub> and CH<sub>4</sub> across Stordalen mire and found that, as per our expectation, these environment-  
293 function relationships changed variably across the thaw gradient, suggesting that correlates of  
294 CO<sub>2</sub> and CH<sub>4</sub> fluxes in transitional stages are not necessarily represented well by correlates of  
295 the end-member or adjacent thaw stages. Contrary to our expectation, we did see significant  
296 trends with thaw in certain bivariate correlations of CH<sub>4</sub> fluxes such as temperature sensitivity,  
297 seasonality and effect of deepening frost table during the growing season. However, these trends  
298 were absent when multiple correlates were considered together, suggesting that dominant  
299 controls on C fluxes and their interactions, change variably as thaw progresses.

### 300 **4.1 Across peatland correlates of C fluxes**

301 Strongest environmental factors associated with the CH<sub>4</sub> flux across all sampled collars were-  
302 elevation, water table depth, pH, VGA, thaw depth and surface water C:N. Each of these  
303 correlates is a possible proxy of one or more controls of temperature, moisture and substrate  
304 quantity and quality on CH<sub>4</sub> flux. Our correlations support previous findings from various  
305 wetland types (as reviewed in Lai, 2009; Olefeldt et al., 2013; Turetsky et al., 2014). The

306 multiple regression of lumped data across Stordalen also showed similar trends to other  
307 temperate, boreal or arctic peatlands. For example, a peatland complex sampled in the  
308 discontinuous permafrost region of Manitoba, Canada by Bubier et al. (1995) showed a best fit  
309 model including WTD, water chemistry and vegetation variables explaining 81% of the variance  
310 in CH<sub>4</sub> fluxes. Bubier et al. (1995) reported WTD as being the strongest individual correlate with  
311 the CH<sub>4</sub> fluxes, but in our best fit model, WTD was not an important variable likely because the  
312 stages with little or no thaw had no water table. Elevation seems to be a better proxy for soil  
313 moisture (and other CH<sub>4</sub> controls), showing the highest contribution to the best fit model (Table  
314 2). Elevation has been previously recognized as an integrator of multiple structural changes  
315 resulting from permafrost thaw and is a potentially useful component of models estimating C  
316 flux in permafrost landscapes (Lee et al., 2011). Rerunning the best fit model without elevation  
317 decreases the overall model fit by 10% but increases the contribution of VGA to the model,  
318 while the contribution of thaw depth and soil temperature remain the same. Removal of elevation  
319 from the model better isolates the relative effects of thaw depth, temperature and VGA on  
320 methane fluxes and suggests that the strongest contribution is from VGA, followed by thaw  
321 depth and soil temperature. VGA is likely a strong effect as it is linked with spatial and seasonal  
322 changes in substrate availability, litter input and root exudates and thus relates to both spatial and  
323 temporal variability in CH<sub>4</sub> flux (Whiting and Chanton 1993).

324 Soil temperature and thaw depth are significant variables in our multiple regression model of  
325 CH<sub>4</sub> flux, while Julian day is not. It may be that across the permafrost gradient, Julian day does  
326 not capture seasonality as well as a combination of thaw depth and soil temperature (Table 2),  
327 suggesting the role of the variable seasonal trajectories of thaw depth and soil temperature in the  
328 different thaw stages, for predicting CH<sub>4</sub> flux.

329 As expected, PAR was the strongest correlate of NEE both in across peatland lumped data and  
330 within thaw stage data. Using the rectangular hyperbola fit, Frohling et al. (1998) reported  
331 parameters from 13 peatland sites wherein PAR explained, on average, 68% (ranging from 47 to  
332 89%) of the variance in NEE. Comparatively our across peatland lumped data fit to the  
333 rectangular hyperbola model explain a lower percent of the variance (52 %) in NEE, likely due  
334 to biases introduced by the high spatial heterogeneity on our site (Laine et al., 2009). WTD,  
335 thaw depth and soil temperature also show significant but weak relationships with CO<sub>2</sub> fluxes.

336 Vascular green area seems to be a better proxy than WTD, thaw depth and soil temperature for  
337 controls on CO<sub>2</sub> fluxes, which makes sense as VGA represents the amount of photosynthesizing  
338 area as well as approximates above and belowground biomass which is related to autotrophic and  
339 heterotrophic respiration (Schneider et al., 2011; Wilson et al., 2006).

#### 340 **4.2 Trends with increasing thaw**

341 Bivariate relationships between correlates and CH<sub>4</sub> flux progress variably as the permafrost  
342 thaws although some significant trends of increasing correlations are seen in soil temperature,  
343 thaw depth and Julian day, as thaw progresses (Fig. 3, 4 and 5). We found that as the permafrost  
344 thaws, temperature sensitivity increases (Fig. 4a), increasing thaw depth has an increasing effect  
345 on CH<sub>4</sub> fluxes (Fig. 4b) and there is a stronger seasonality effect (Fig. 4c). This trend of  
346 increasing correlation could be partly due to the increasing magnitude and variance of not only  
347 CH<sub>4</sub> fluxes but also the environmental variables with thawing permafrost. Additionally, higher  
348 VGA later in the growing season could also be result in a stronger seasonality effect (Fig. 4c) in  
349 the later stages of thaw, especially as these stages had the highest sedge VGA. The Arrhenius  
350 plots of soil temperature and CH<sub>4</sub> fluxes showed increased temperature sensitivity from less  
351 thawed to more thawed stages, with the slope and R<sup>2</sup> of this regression increasing (Fig. 5).  
352 Changing temperature sensitivity in our results contradicts results from Yvon-Durocher et al.  
353 (2014) that suggest a consistent temperature sensitivity of CH<sub>4</sub> fluxes across scales. Apparent  
354 temperature sensitivity can be confounded due to changes in substrate availability (Kirschbaum,  
355 2006). Increasing temperature sensitivity with thaw in our results could be related to higher  
356 substrate availability (supported by higher VGA) in thawed stages switching CH<sub>4</sub> production  
357 from being substrate limited to becoming temperature limited. Lower temperature sensitivity in  
358 the intact permafrost could also be related to DOC quality. Olefeldt et al. (2012) report higher  
359 aromaticity in DOC exported from palsa and bog catchments at Stordalen compared to fen  
360 catchments and a high proportion of aromatic compounds in litter is generally associated with  
361 decreased temperature sensitivity (eg. Erhagen et al., 2013). High temperature sensitivity in  
362 wetter sites has also been reported by Olefeldt et al. (2013) in a meta-analysis of CH<sub>4</sub> emissions  
363 from terrestrial ecosystems worldwide. Christensen et al. (2003) found that temperature is a  
364 limiting factor only when the WTD is 10 cm or less below the surface, whereas a lower WTD is  
365 more sensitive to WTD fluctuations than to soil temperature fluctuations. This is generally

366 supported in our results with stages 4 to 6 that have growing season mean WTD greater than 10  
367 cm (Table 1) having lower sensitivity to WTD than stages 7 to 10, though there is variability in  
368 both classes (Fig. 3). Our estimated temperature sensitivity for each thaw stage is the net effect  
369 of temperature on methanogenesis and methanotrophy and since we only measure the net CH<sub>4</sub>  
370 flux we cannot isolate the relative temperature sensitivities for the two processes. Also  
371 interesting is the effect of the increasing thaw, over the growing season, on CH<sub>4</sub> flux- more  
372 significant in the wetter more thawed stages than the drier intact permafrost stages (Fig. 3 and  
373 4b). A similar trend was also emphasized in Olefeldt et al. (2013). The deepening frost table is  
374 related to temperature and thus could also represent the larger temperature sensitivity of CH<sub>4</sub> in  
375 later thaw stages. Additionally, larger variance in thaw depths of later thaw stages could explain  
376 the larger effect of thaw depth in these stages. The larger variance in thaw depth could be  
377 attributed to a steeper drop in thaw depths as the growing season progresses in the wetter thaw  
378 stages due to the dependence of thermal conductivity of peat on the degree of wetness (Quinton  
379 et al. 2009).

380 While bivariate relationships between correlates and C flux provide insight into the possible  
381 controls on these fluxes, multiple regressions better demonstrate the interactive nature of these  
382 correlates. Re-running the best fit model of the lumped data (Table 2) for each thaw stage  
383 showed that the strength of the overall model and the parameter estimates are variable along the  
384 thaw gradient (Fig. 6). While elevation had a strong effect in across peatland lumped data, it  
385 makes sense that it was a significant effect only for a few within thaw stage analyses (thaw  
386 stages 1, 4, 8 and 9) because these stages had diverse habitats with spatially varying elevations.  
387 Soil Temperature was not a statistically significant estimate for any of the thaw stages, possibly  
388 because elevation and thaw depth are better proxies for the long term thermal regime and also  
389 relate to several other controls of CH<sub>4</sub> flux, as previously mentioned. VGA was only a significant  
390 effect within thaw stages 8 and 9. These results emphasize that spatial differences in elevation  
391 are not as important within thaw stages as they were in across peatland lumped data. Also, thaw  
392 depth and VGA have variable effects but generally stronger in the thawed stages.

393 Similar to CH<sub>4</sub> flux, the strength of the major correlate for CO<sub>2</sub> flux (PAR) changes variably  
394 across the thaw gradient. While the across peatland relationship of NEE with temperature and  
395 PAR is weaker than that found in other peatland sites (e.g. Bubier et al., 2003), when broken

396 down into thaw stages, the percent variance of NEE explained increases (up to 91%; Table 4) for  
397 many thaw stages. The sample size for each thaw stages is different making it problematic to  
398 statistically compare the thaw stages. However, we found that the  $R^2$  is not significantly  
399 correlated to the sample size for that thaw stage, suggesting that there are other factors increasing  
400 the control of PAR on NEE as permafrost thaws such as increased photosynthesizing biomass  
401 (reflected by increasing VGA and GPP). If VGA is no longer limiting, PAR sensitivity could be  
402 increasing as permafrost thaws. This is supported in the parameter fitting for each thaw stage  
403 (Table 4), the general trends observed are that the  $\text{CO}_2$  fixed at maximum PAR ( $GP_{MAX}$ )  
404 increases as permafrost thaws as does the amount of  $\text{CO}_2$  fixed per unit of PAR ( $\alpha$ ), both of  
405 which could be related to increase in VGA but also the photosynthetic capacity change from  
406 plant species changes. The amount of respiration at  $0^\circ\text{C}$  generally increases with thaw, which  
407 could be related to increasing substrate availability. Trends of increasing GPP and ecosystem  
408 respiration with permafrost thaw have been reported in previous studies (eg. Dorrepaal et al.,  
409 2009; Hicks Pries et al., 2013). However, in our results these trends are not significant along the  
410 thaw gradient and progress variably.

#### 411 **4.3 Relationship between NEE and $\text{CH}_4$**

412 NEE is thought to be related to  $\text{CH}_4$  emissions due to the shared association with recently  
413 produced substrate availability, root exudates and turnover and litter input, and this link has been  
414 observed in several studies (Bellisario et al., 1999; Ström and Christensen, 2007; Whiting and  
415 Chanton, 1993, etc.). In our thaw stages, there was also an overall significant and positive  
416 relationship between growing season averages of  $GP_{MAX}$  and  $\text{CH}_4$  ( $\rho=0.56$ ,  $p=0.0021$ ; Fig. 7).  
417 Interestingly, thaw stages 8 to 10 (graminoid dominated) have a different relationship of  $GP_{MAX}$   
418 and  $\text{CH}_4$  compared with thaw stages 1 to 7 (moss dominated) suggesting a shift in the  
419 partitioning of C loss from the system as  $\text{CO}_2$  or  $\text{CH}_4$  with increasing thaw and changing  
420 vegetation. We expected this shift to be related to an increase in graminoid VGA (increase in  
421 lability and  $\text{CH}_4$  emission via aerenchyma), which was supported by our data. Surprisingly, we  
422 also found the shift to be related to a loss of *Sphagnum* cover, perhaps due to an increase in pH  
423 and decrease in organic matter lability. Furthermore, there was a significant interaction between  
424 soil temperature and *Sphagnum* cover in a linear model explaining  $\text{CH}_4:\text{CO}_2$ , suggesting that the

425 relationship of CH<sub>4</sub> and CO<sub>2</sub> depends on *Sphagnum* abundance but the effect of *Sphagnum* varies  
426 by temperature (Table 5).

#### 427 **4.4 Variable changes in ecosystem relationships with increasing thaw**

428 Permafrost thaw increases magnitude and variance of CO<sub>2</sub> and CH<sub>4</sub> fluxes as well as changes the  
429 abiotic and biotic correlates of these fluxes. As a result, the relationships between the correlates  
430 and C fluxes change. While in the lumped across peatland data, spatially variable factors are the  
431 dominant correlates of CO<sub>2</sub> and CH<sub>4</sub> fluxes (elevation being the best proxy for thermal regime,  
432 soil moisture, VGA, etc.), within thaw stages it is the correlates with high temporal variations  
433 that play a critical role (Julian day, deepening frost table and soil temperature). The changing  
434 correlates of CO<sub>2</sub> and CH<sub>4</sub> fluxes are important to consider from a context of upscaling these  
435 processes from within thaw stage to site to landscape scales. Changing sensitivity of CH<sub>4</sub> fluxes  
436 to temperature, likely related to a shift from substrate to temperature limitation going from low  
437 biomass and low nutrient palsa stages to high biomass and high nutrient thawed stages. Based  
438 on the range of temperature response curves of CH<sub>4</sub> flux across the thaw gradient (Fig. 4a),  
439 applying one activation energy value to estimate landscape level CH<sub>4</sub> fluxes at Stordalen would  
440 not be appropriate and would likely require a set of parameterizations for the various thaw  
441 stages. Variable temperature sensitivities to C fluxes have been recognized in major thaw stages  
442 in the past (eg. Lupascu and Wadham, 2012), but our study demonstrates that this variability is  
443 present even in the transitional stages. Furthermore, the multiple regression analyses for each  
444 thaw stages (Fig. 6) demonstrated the changing relative importance and interactive effects of  
445 dominant correlates of CH<sub>4</sub> flux highlighting that controls in transitional stages of permafrost  
446 thaw are not necessarily related to controls in adjacent or end-member stages.

447 Paleo-ecological methods were not employed to confirm the actual thaw status of the thaw stages  
448 used in our analyses. Rather, our space for time approach was employed to sample the major  
449 stages of thaw at Stordalen acknowledged in previous studies (Bäckstrand et al., 2010; Johansson  
450 et al., 2006; Svensson et al., 1999, etc.)- encompassing palsa (our stages 1 to 3), internal fen (our  
451 stages 4 to 6), completely thawed flow through fen (our stages 7 to 10) type habitats- while  
452 capturing the wide range of structural conditions within each one of these 3 broad thaw stages.  
453 We acknowledge that structural changes due to thaw may progress variably and tried to capture  
454 each of these pathways. For example, palsa may collapse abruptly into a wet sedge dominated

455 habitat that then switches to a *Sphagnum* lawn (our thaw stage 1 progressing into stage 8 and  
456 then to stage 5). Alternatively, this progression can be gradual with a decrease in elevation of  
457 palsa (stage 1 to 2 and then 3), followed by progression into *Sphagnum* lawn (stage 4 and 5).  
458 Regardless, the focus of our study was the changing correlates of C fluxes along the thaw  
459 gradient and a proposed sequence of thaw stages was required to analyze these changes.

## 460 **5 Conclusions**

461 Our results on the environmental correlates of C fluxes interacting and changing variably with  
462 thaw suggest that using process based models or relationships between NEE and CH<sub>4</sub> flux to  
463 derive landscape level C fluxes would require additional information about transitional thaw  
464 stages.

465 Peatlands in the discontinuous permafrost zone are highly heterogeneous, especially if they are  
466 actively thawing. Our research highlights the variability observed in structure-function  
467 relationships with permafrost thaw. Additionally, by identifying across peatland structure-  
468 function relationships that are maintained across the heterogeneous landscape our results will  
469 assist in improving regional estimates of the carbon balance and provide insight into the level of  
470 aggregation or disaggregation needed in models to capture ecosystem level response to change.

## 471 **Acknowledgements**

472 We gratefully acknowledge valuable equipment, lab and field assistance from Tom Parker, Silvie  
473 Harder, Étienne Fluet-Chouinard, Paul Wilson, Christina Puzzolo, Mike Dalva, Patrick Crill,  
474 Ruth Varner, Samantha Werner, Carmody McCalley and Niklas Rakos and elevation data from  
475 Andreas Persson. We also thank the staff at Abisko Scientific Research Station, Sweden. The  
476 research was supported by a James McGill Professorship Stipend to N.T.R, a Discovery Grant  
477 and a Strategic Project Grant from the Natural Sciences and Engineering Research Council of  
478 Canada (NSERC) to N.T.R. The research was also supported by the Global Environmental and  
479 Climate Change Regroupement stratégique graduate stipend to A.M. funded by the Fonds de  
480 recherche du Québec – Nature et technologies (FQRNT), McGill University Geography  
481 Department funding to A. M. and a PhD research scholarship to A. M. from FQRNT.

## 482 **References**

- 483 Bäckstrand, K., Crill, P. M., Jackowicz-Korczyński, M., Mastepanov, M., Christensen, T. R. and  
484 Bastviken, D.: Annual carbon gas budget for a subarctic peatland, Northern Sweden,  
485 *Biogeosciences*, 7(1), 95–108, doi:10.5194/bg-7-95-2010, 2010.
- 486 Bellisario, L., Bubier, J. L. and Moore, T.: Controls on CH<sub>4</sub> emissions from a northern peatland,  
487 *Global Biogeochem. Cycles*, 13(1), 81–91, 1999.
- 488 Belshe, E. F., Schuur, E. A. G., Bolker, B. M. and Bracho, R.: Incorporating spatial  
489 heterogeneity created by permafrost thaw into a landscape carbon estimate, *J. Geophys. Res.*,  
490 117(G1), G01026, doi:10.1029/2011JG001836, 2012.
- 491 Bubier, J. L., Bhatia, G., Moore, T., Roulet, N. and Lafleur, P.: Spatial and temporal variability  
492 in growing-season net ecosystem carbon dioxide exchange at a large peatland in Ontario,  
493 Canada, *Ecosystems*, 6(4), 353–367, doi:10.1007/s, 2003.
- 494 Bubier, J. L., Moore, T. R., Bellisario, L., Comer, N. T. and Crill, P. M.: Ecological controls on  
495 methane emissions from a northern peatland complex in the zone of discontinuous permafrost,  
496 Manitoba, Canada, *Global Biogeochem. Cycles*, 9(4), 455–470, 1995.
- 497 Callaghan, T. V., Bergholm, F., Christensen, T. R., Jonasson, C., Kokfelt, U. and Johansson, M.:  
498 A new climate era in the sub-Arctic: Accelerating climate changes and multiple impacts,  
499 *Geophys. Res. Lett.*, 37(14), 1–6, doi:10.1029/2009GL042064, 2010.
- 500 Camill, P.: Patterns of boreal permafrost peatland vegetation across environmental gradients  
501 sensitive to climate warming, *Can. J. Bot.*, 77, 721–733, 1999.
- 502 Camill, P.: Permafrost Thaw Accelerates in Boreal Peatlands During Late-20th Century Climate  
503 Warming, *Clim. Change*, 68(1-2), 135–152, doi:10.1007/s10584-005-4785-y, 2005.
- 504 Camill, P., Lynch, J. A., Clark, J. S., Adams, J. B. and Jordan, B.: Changes in Biomass,  
505 Aboveground Net Primary Production, and Peat Accumulation following Permafrost Thaw in the  
506 Boreal Peatlands of Manitoba, Canada, *Ecosystems*, 4(5), 461–478, 2001.
- 507 Christensen, T. R., Ekberg, A., Ström, L., Mastepanov, M., Panikov, N., Oquist, M., Svensson,  
508 B. H., Nykänen, H., Martikainen, P. J. and Oskarsson, H.: Factors controlling large scale  
509 variations in methane emissions from wetlands, *Geophys. Res. Lett.*, 30(7), 1414,  
510 doi:10.1029/2002GL016848, 2003.
- 511 Christensen, T. R., Johansson, T. R., Akerman, H. J., Mastepanov, M., Malmer, N., Friborg, T.,  
512 Crill, P., and Svensson, B. H.: Thawing sub-arctic permafrost: Effects on vegetation and methane  
513 emissions, *Geophys. Res. Lett.*, 31, L04501, doi:10.1029/2003GL018680, 2004.
- 514 Dorrepaal, E., Toet, S., van Logtestijn, R. S. P., Swart, E., van de Weg, M. J., Callaghan, T. V.  
515 and Aerts, R.: Carbon respiration from subsurface peat accelerated by climate warming in the  
516 subarctic, *Nature*, 460(7255), 616–619, doi:10.1038/nature08216, 2009.

- 517 Erhagen, B., Öquist, M., Sparrman, T., Haei, M., Ilstedt, U., Hedenström, M., Schleucher, J. and  
518 Nilsson, M. B.: Temperature response of litter and soil organic matter decomposition is  
519 determined by chemical composition of organic material., *Glob. Chang. Biol.*, 19(12), 3858–71,  
520 doi:10.1111/gcb.12342, 2013.
- 521 Frohling, S., Bubier, J. L., Moore, T., Ball, T., Bellisario, L., Bhardwaj, A., Carroll, P., Crill, P.,  
522 Lafleur, P., McCaughey, J. H., Roulet, N., Suyker, A., Verma, S., Waddington, J. and Whiting,  
523 G.: Relationship between ecosystem productivity and photosynthetically active radiation for  
524 northern peatlands, *Global Biogeochem. Cycles*, 21(1), 115–126, 1998.
- 525 Hicks Pries, C. E., Schuur, E. A. G. and Crummer, K. G.: Thawing permafrost increases old soil  
526 and autotrophic respiration in tundra: partitioning ecosystem respiration using  $\delta(13) C$  and  $\Delta(14)$   
527 C., *Glob. Chang. Biol.*, 19(2), 649–61, doi:10.1111/gcb.12058, 2013.
- 528 Hines, M. E., Duddleston, K. N., Rooney-Varga, J. N., Fields, D. and Chanton, J. P.: Uncoupling  
529 of acetate degradation from methane formation in Alaskan wetlands: Connections to vegetation  
530 distribution, *Global Biogeochem. Cycles*, 22(2), 1–12, doi:10.1029/2006GB002903, 2008.
- 531 Hodgkins, S. B., Tfaily, M. M., McCalley, C. K., Logan, T. A., Crill, P. M., Saleska, S. R., Rich,  
532 V. I. and Chanton, J. P.: Changes in peat chemistry associated with permafrost thaw increase  
533 greenhouse gas production., *Proc. Natl. Acad. Sci. U. S. A.*, 111(16), 5819–24,  
534 doi:10.1073/pnas.1314641111, 2014.
- 535 Johansson, T., Malmer, N., Crill, P. M., Friborg, T., Åkerman, J. H., Mastepanov, M. and  
536 Christensen, T. R.: Decadal vegetation changes in a northern peatland, greenhouse gas fluxes and  
537 net radiative forcing, *Glob. Chang. Biol.*, 12(12), 2352–2369, doi:10.1111/j.1365-  
538 2486.2006.01267.x, 2006.
- 539 Kirschbaum, M.: The temperature dependence of organic-matter decomposition—still a topic of  
540 debate, *Soil Biol. Biochem.*, 38(9), 2510–2518, doi:10.1016/j.soilbio.2006.01.030, 2006.
- 541 Kvillner, E. and Sonesson, M.: Plant Distribution and Environment of a Subarctic Mire, *Ecol.*  
542 *Bull.*, (30), 97–111, 1980.
- 543 Lai, D. Y. F.: Methane Dynamics in Northern Peatlands: A Review, *Pedosphere*, 19(4), 409–421,  
544 doi:10.1016/S1002-0160(09)00003-4, 2009.
- 545 Lai, Y. F.: Spatial and Temporal Variations of Carbon Dioxide and Methane Fluxes Measured by  
546 Autochambers at the Mer Bleue Bog, PhD thesis. McGill University, Montreal, Canada., 2012.
- 547 Laine, A., Riutta, T., Juutinen, S., Välijärvi, M. and Tuittila, E.-S. Acknowledging the spatial  
548 heterogeneity in modelling/reconstructing carbon dioxide exchange in a northern aapa mire,  
549 *Ecol. Modell.*, 220(20), 2646–2655, doi:10.1016/j.ecolmodel.2009.06.047, 2009.

550 Lee, H., Schuur, E. A. G., Inglett, K. S., Lavoie, M. and Chanton, J. P.: The rate of permafrost  
551 carbon release under aerobic and anaerobic conditions and its potential effects on climate, *Glob.*  
552 *Chang. Biol.*, 18(2), 515–527, doi:10.1111/j.1365-2486.2011.02519.x, 2012.

553 Lee, H., Schuur, E. A. G., Vogel, J. G., Lavoie, M., Bhadra, D. and Staudhammer, C. L.: A  
554 spatially explicit analysis to extrapolate carbon fluxes in upland tundra where permafrost is  
555 thawing, *Glob. Chang. Biol.*, 17(3), 1379–1393, doi:10.1111/j.1365-2486.2010.02287.x, 2011.

556 Luoto, M., Heikkinen, R. K. and Carter, T. R.: Loss of palusa mires in Europe and biological  
557 consequences, *Environ. Conserv.*, 31(1), 30–37, doi:10.1017/S0376892904001018, 2004.

558 Lupascu, M. and Wadham, J.: Temperature sensitivity of methane production in the permafrost  
559 active layer at Stordalen, Sweden: A comparison with non-permafrost northern wetlands, *Arctic,*  
560 *Antarct. Alp. Res.*, 44(4), 469–482, 2012.

561 Mackelprang, R., Waldrop, M. P., DeAngelis, K. M., David, M. M., Chavarria, K. L., Blazewicz,  
562 S. J., Rubin, E. M. and Jansson, J. K.: Metagenomic analysis of a permafrost microbial  
563 community reveals a rapid response to thaw., *Nature*, 480(7377), 368–71,  
564 doi:10.1038/nature10576, 2011.

565 Malmer, N., Johansson, T., Olsrud, M. and Christensen, T. R.: Vegetation, climatic changes and  
566 net carbon sequestration in a North-Scandinavian subarctic mire over 30 years, *Glob. Chang.*  
567 *Biol.*, 11, 1895–1909, doi:10.1111/j.1365-2486.2005.01042.x, 2005.

568 McCalley, C., Woodcroft, B., Hodgkins, S., Wehr, R., Kim, E.-H., Mondav, R., Crill, P.,  
569 Chanton, J., Rich, V., Tyson, G. and Saleska, S.: Methane dynamics regulated by microbial  
570 community response to permafrost thaw, *Nature*, 514, 478–481, doi:10.1038/nature13798, 2014.

571 McConnell, N. A., Turetsky, M. R., David McGuire, A., Kane, E. S., Waldrop, M. P. and  
572 Harden, J. W.: Controls on ecosystem and root respiration across a permafrost and wetland  
573 gradient in interior Alaska, *Environ. Res. Lett.*, 8(4), 045029, doi:10.1088/1748-  
574 9326/8/4/045029, 2013.

575 Morrissey, L. and Livingston, G.: Methane emissions from Alaska arctic tundra: An assessment  
576 of local spatial variability, *J. Geophys. Res.*, 97(92), 661–670, 1992.

577 Olefeldt, D. and Roulet, N. T.: Effects of permafrost and hydrology on the composition and  
578 transport of dissolved organic carbon in a subarctic peatland complex, *J. Geophys. Res.*,  
579 117(G1), G01005, doi:10.1029/2011JG001819, 2012.

580 Olefeldt, D. and Roulet, N. T.: Permafrost conditions in peatlands regulate magnitude, timing,  
581 and chemical composition of catchment dissolved organic carbon export., *Glob. Chang. Biol.*,  
582 20: 3122–3136, doi:10.1111/gcb.12607, 2014.

- 583 Olefeldt, D., Turetsky, M. R., Crill, P. M. and McGuire, A. D.: Environmental and physical  
584 controls on northern terrestrial methane emissions across permafrost zones., *Glob. Chang. Biol.*,  
585 19(2), 589–603, doi:10.1111/gcb.12071, 2013.
- 586 Osterkamp, T.: The recent warming of permafrost in Alaska, *Glob. Planet. Change*, 49(3-4),  
587 187–202, doi:10.1016/j.gloplacha.2005.09.001, 2005.
- 588 Quinton, W., Hayashi, M. and Chasmer, L.: Peatland hydrology of discontinuous permafrost in  
589 the Northwest Territories: overview and synthesis, *Can. Water Resour. J.*, 34(4), 311–328, 2009.
- 590 Schneider, J., Kutzbach, L. and Wilmking, M.: Carbon dioxide exchange fluxes of a boreal  
591 peatland over a complete growing season, Komi Republic, NW Russia, *Biogeochemistry*, 111(1-  
592 3), 485–513, doi:10.1007/s10533-011-9684-x, 2011.
- 593 Schuur, E. A. G., Abbott, B. W., Bowden, W. B., Brovkin, V., Camill, P., Canadell, J. G.,  
594 Chanton, J. P., Chapin, F. S., Christensen, T. R., Ciais, P., Crosby, B. T., Czimczik, C. I., Grosse,  
595 G., Harden, J., Hayes, D. J., Hugelius, G., Jastrow, J. D., Jones, J. B., Kleinen, T., Koven, C. D.,  
596 Krinner, G., Kuhry, P., Lawrence, D. M., McGuire, a. D., Natali, S. M., O'Donnell, J. a., Ping,  
597 C. L., Riley, W. J., Rinke, A., Romanovsky, V. E., Sannel, a. B. K., Schädel, C., Schaefer, K.,  
598 Sky, J., Subin, Z. M., Tarnocai, C., Turetsky, M. R., Waldrop, M. P., Walter Anthony, K. M.,  
599 Wickland, K. P., Wilson, C. J. and Zimov, S. a.: Expert assessment of vulnerability of permafrost  
600 carbon to climate change, *Clim. Change*, 119(2), 359–374, doi:10.1007/s10584-013-0730-7,  
601 2013.
- 602 Schuur, E. A. G., Bockheim, J., Canadell, J. G., Euskirchen, E., Field, C. B., Goryachkin, S. V.,  
603 Hagemann, S., Kuhry, P., Lafleur, P. M., Lee, H., Mazhitova, G., Nelson, F. E., Rinke, A.,  
604 Romanovsky, V. E., Shiklomanov, N., Tarnocai, C., Venevsky, S., Vogel, J. G. and Zimov, S. a.:  
605 Vulnerability of Permafrost Carbon to Climate Change: Implications for the Global Carbon  
606 Cycle, *Bioscience*, 58(8), 701-714, doi:10.1641/B580807, 2008.
- 607 Sitch, S., McGuire, A. and Kimball, J.: Assessing the carbon balance of circumpolar Arctic  
608 tundra using remote sensing and process modeling, *Ecol. Appl.*, 17(1), 213–234, 2007.
- 609 Smith, L. C., Beilman, D. W., Kremenetski, K. V., Sheng, Y., MacDonald, G. M., Lammers, R.  
610 B., Shiklomanov, A. I. and Lapshina, E. D.: Influence of permafrost on water storage in West  
611 Siberian peatlands revealed from a new database of soil properties, *Permafr. Periglac. Process.*,  
612 23(1), 69–79, doi:10.1002/ppp.735, 2012.
- 613 Ström, L. and Christensen, T. R.: Below ground carbon turnover and greenhouse gas exchanges  
614 in a sub-arctic wetland, *Soil Biol. Biochem.*, 39(7), 1689–1698,  
615 doi:10.1016/j.soilbio.2007.01.019, 2007.
- 616 Svensson, B. H., Christensen, T. R., Johansson, E. and Oquist, M.: Interdecadal Changes in CO<sub>2</sub>  
617 and CH<sub>4</sub> Fluxes of a Subarctic Mire: Stordalen Revisited after 20 Years, *Oikos*, 85(1), 22-30,  
618 doi:10.2307/3546788, 1999.

- 619 Tarnocai, C., Canadell, J. G., Schuur, E. A. G., Kuhry, P., Mazhitova, G. and Zimov, S.: Soil  
620 organic carbon pools in the northern circumpolar permafrost region, *Global Biogeochem. Cycles*,  
621 23, GB2023, doi:10.1029/2008GB003327, 2009.
- 622 Treat, C. C., Wollheim, W. M., Varner, R. K., Grandy, A. S., Talbot, J. and Frolking, S.:  
623 Temperature and peat type control CO<sub>2</sub> and CH<sub>4</sub> production in Alaskan permafrost peats., *Glob.*  
624 *Chang. Biol.*, 20(8), 2674–86, doi:10.1111/gcb.12572, 2014.
- 625 Turetsky, M. R.: Decomposition and Organic Matter Quality in Continental Peatlands: The  
626 Ghost of Permafrost Past, *Ecosystems*, 7(7), 740–750, doi:10.1007/s10021-004-0247-z, 2004.
- 627 Turetsky, M. R., Kotowska, A., Bubier, J. L., Dise, N. B., Crill, P., Hornibrook, E. R. C.,  
628 Minkinen, K., Moore, T. R., Myers-Smith, I. H., Nykänen, H., Olefeldt, D., Rinne, J., Saarnio,  
629 S., Shurpali, N., Tuittila, E.-S., Waddington, J. M., White, J. R., Wickland, K. P. and Wilmking,  
630 M.: A synthesis of methane emissions from 71 northern, temperate, and subtropical wetlands.,  
631 *Glob. Chang. Biol.*, 20(7), 2183–97, doi:10.1111/gcb.12580, 2014.
- 632 Turetsky, M. R., Wieder, R. K., Vitt, D. H., Evans, R. J. and Scott, K. D.: The disappearance of  
633 relict permafrost in boreal north America: Effects on peatland carbon storage and fluxes, *Glob.*  
634 *Chang. Biol.*, 13(9), 1922–1934, doi:10.1111/j.1365-2486.2007.01381.x, 2007.
- 635 Vitt, D. H., Halsey, L. A. and Zoltai, S. C.: The changing landscape of Canada’s western boreal  
636 forest: the current dynamics of permafrost, *Can. J. For. Res.*, 30(2), 283–287, doi:10.1139/cjfr-  
637 30-2-283, 2000.
- 638 Vogel, J., Schuur, E. A. G., Trucco, C. and Lee, H.: Response of CO<sub>2</sub> exchange in a tussock  
639 tundra ecosystem to permafrost thaw and thermokarst development, *J. Geophys. Res.*, 114(G4),  
640 G04018, doi:10.1029/2008JG000901, 2009.
- 641 Whiting, G. and Chanton, J.: Primary production control of methane emission from wetlands,  
642 *Nature*, 364, 794–795, 1993.
- 643 Wilson, D., Alm, J., Riutta, T., Laine, J., Byrne, K. A., Farrell, E. P. and Tuittila, E.-S.: A high  
644 resolution green area index for modelling the seasonal dynamics of CO<sub>2</sub> exchange in peatland  
645 vascular plant communities, *Plant Ecol.*, 190(1), 37–51, doi:10.1007/s11258-006-9189-1, 2006.
- 646 Ye, R., Jin, Q., Bohannon, B., Keller, J. K., McAllister, S. A. and Bridgman, S. D.: pH controls  
647 over anaerobic carbon mineralization, the efficiency of methane production, and methanogenic  
648 pathways in peatlands across an ombrotrophic–minerotrophic gradient, *Soil Biol. Biochem.*, 54,  
649 36–47, doi:10.1016/j.soilbio.2012.05.015, 2012.
- 650 Yvon-Durocher, G., Allen, A. P., Bastviken, D., Conrad, R., Gudas, C., St-Pierre, A., Thanh-  
651 Duc, N. and del Giorgio, P. a: Methane fluxes show consistent temperature dependence across  
652 microbial to ecosystem scales., *Nature*, 507(7493), 488–91, doi:10.1038/nature13164, 2014.

653 Zhang, Y., Sachs, T., Li, C. and Boike, J.: Upscaling methane fluxes from closed chambers to  
654 eddy covariance based on a permafrost biogeochemistry integrated model, *Glob. Chang. Biol.*,  
655 18(4), 1428–1440, doi:10.1111/j.1365-2486.2011.02587.x, 2012.

656

657

658

659

660

661

662

663

664

665

666

667

668

669

670

671

672

673

674

675

676

677

678

679 **6 Tables**

680 **Table 1.** Details of each thaw stage- habitat description and dominant vegetation, vascular plant  
 681 green area (VGA), presence or absence of permafrost, mean growing season water table depth  
 682 (from 19 days of sampling over 2 years), mean surface water pH, reduced conductivity (Cond)  
 683 and C:N ratio, growing season mean soil temperature at 10 cm depth below surface and mean  
 684 growing season CH<sub>4</sub> fluxes. Details on CO<sub>2</sub> flux for each thaw stage can be found in Table 4.  
 685 WTD was only reported for stages with a water table on more than 5 sampled days. All values  
 686 reported after ± are standard errors.

Thaw Stage	Habitat description and dominant vegetation	Mean VGA (cm <sup>2</sup> )	Perma-frost	Mean WTD (cm)	pH	Cond (mg L <sup>-1</sup> )	C:N	Mean Soil temperature (°C)	Mean CH <sub>4</sub> flux (mg m <sup>-2</sup> day <sup>-1</sup> )
1	Intact palsa, <i>Dicranum elongatum</i> , <i>Vaccinium uliginosum</i>	279.6	✓	-	-	-	-	6.2±0.2	-1.3±0.2
2	Slightly thawing palsa, <i>D. elongatum</i> , <i>Eriophorum vaginatum</i> , <i>Ptillidium ciliare</i>	232.7	✓	-	-	-	-	6.7±0.2	7.1±1.1
3	Collapsing palsa, desiccated <i>Sphagnum fuscum</i> , lichens, <i>Andromeda polifolia</i>	66.7	✓	-	-	-	-	6.6±0.2	-1.1±0.3
4	<i>Sphagnum</i> lawn in transition between stage 3 and 5	54.0	-	-11.6±1.3	-	-	-	8.3±0.3	7.6±1.4
5	<i>Sphagnum</i> lawn	60.3	-	-10.1±0.7	4.0	8.0	35.8	7.2±0.3	18.7±2.7
6	<i>Sphagnum</i> lawn, <i>Betula nana</i>	312.1	-	-11.5±0.6	-	-	-	8.1±0.4	29.5±4.8
7	<i>E. vaginatum</i> , <i>S. cuspidatum</i> , open water	334.4	-	-2.3±0.6	4.1	17.0	45.3	9.9±0.3	56.5±3.5
8	<i>E. vaginatum</i> , <i>Drepanocladus schulzei</i> , open water	322.0	-	1.8±0.9	4.0	76.2	47.9	10.4±0.3	102.4±7.5
9	<i>Eriophorum angustifolium</i> , open water	1136.3	-	2.3±0.6	4.5	30.0	46.6	7.6±0.3	370.2±52.1
10	<i>Polytrichum jensenii</i> , <i>Carex rostrata</i>	1528.7	-	-5.8±1.3	4.7	22.6	53.0	7.2±0.3	266.2±22.7

687

688

689

690

691

692 **Table 2.** Multiple regression model between environmental variables and CH<sub>4</sub> flux across the  
 693 site. Listed environmental variables explain 73% of the variance in CH<sub>4</sub> flux ( $R^2 = 0.73$ ,  $F_{4,391}$   
 694  $=267.1$ ,  $p < 0.0001$ )

Term	Estimate	Std Error	t Ratio	Prob> t
Intercept	344.38	26.94	12.8	<.0001
Elevation	-0.98	0.077	-12.8	<.0001
Soil temp	0.031	0.007	4.43	<.0001
Thaw depth	-0.005	0.001	-8.50	<.0001
VGA	0.001	0.000	7.09	<.0001

695  
 696  
 697  
 698  
 699  
 700  
 701  
 702  
 703  
 704  
 705  
 706  
 707  
 708  
 709  
 710  
 711  
 712  
 713

714 **Table 3.** Abiotic and biotic relationships with Gross Primary Production ( $GPP = NEE - R_{eco}$ ), Net  
 715 Ecosystem Exchange (NEE) and Ecosystem Respiration ( $R_{eco}$ ).  $R_{eco}$  has negative values and  
 716 therefore, negative correlation signifies that larger VGA or Soil temp have higher  $R_{eco}$ . Similarly,  
 717 since thaw depth has negative values, negative correlations with GPP and NEE mean that deeper  
 718 frost tables relate to greater GPP and NEE.

Function	Correlate	Spearman's $\rho$	p-value
NEE	Thaw Depth	-0.21	0.0058
NEE	Soil Temp	0.14	0.0112
NEE	WTD	0.24	0.0002
NEE	VGA	0.58	0.0180
GPP	Thaw Depth	-0.29	0.0020
GPP	WTD	0.20	0.0177
$R_{eco}$	Soil Temp	-0.16	0.0226
$R_{eco}$	VGA	-0.56	0.0250

719  
 720  
 721  
 722  
 723  
 724  
 725  
 726  
 727  
 728  
 729  
 730  
 731  
 732  
 733

734 **Table 4.** Parameter estimates  $\pm$  standard error from rectangular hyperbola fit of NEE and PAR.  
 735 PAR dependence of NEE generally increases and becomes more significant from less to more  
 736 thawed stages as shown by the adjusted  $R^2$  ( $p < 0.0001$  for all thaw stages). There is a general  
 737 trend of increasing,  $GP_{MAX}$ , alpha and A, going from less thawed to more thawed stages.

Thaw Stage	$GP_{MAX}$ ( $\mu\text{mol CO}_2 \text{ m}^{-2} \text{ s}^{-1}$ )	$\alpha$ ( $\frac{\mu\text{mol CO}_2 \text{ m}^{-2} \text{ s}^{-1}}{\mu\text{mol PAR m}^{-2} \text{ s}^{-1}}$ )	A ( $\mu\text{mol CO}_2 \text{ m}^{-2} \text{ s}^{-1}$ )	$R^2$	n
1	3.85 $\pm$ 1.21		-4.36 $\pm$ 0.53	0.59	26
2	3.99 $\pm$ 0.53	0.015 $\pm$ 0.004	-1.72 $\pm$ 0.16	0.71	75
3	2.82 $\pm$ 0.61	0.008 $\pm$ 0.003	-1.52 $\pm$ 0.13	0.80	26
4	2.44 $\pm$ 0.31	0.014 $\pm$ 0.005	-0.89 $\pm$ 0.11	0.76	52
5	3.87 $\pm$ 0.30	0.030 $\pm$ 0.007	-1.28 $\pm$ 0.11	0.85	78
6	5.15 $\pm$ 0.52	0.053 $\pm$ 0.021	-2.76 $\pm$ 0.25	0.89	27
7	6.28 $\pm$ 0.72	0.032 $\pm$ 0.010	-1.79 $\pm$ 0.24	0.74	78
8	2.15 $\pm$ 0.24	0.015 $\pm$ 0.005	-0.94 $\pm$ 0.09	0.82	98
9	8.16 $\pm$ 0.86	0.072 $\pm$ 0.023	-3.49 $\pm$ 0.32	0.91	27
10	6.62 $\pm$ 1.34		-5.35 $\pm$ 0.82	0.69	18

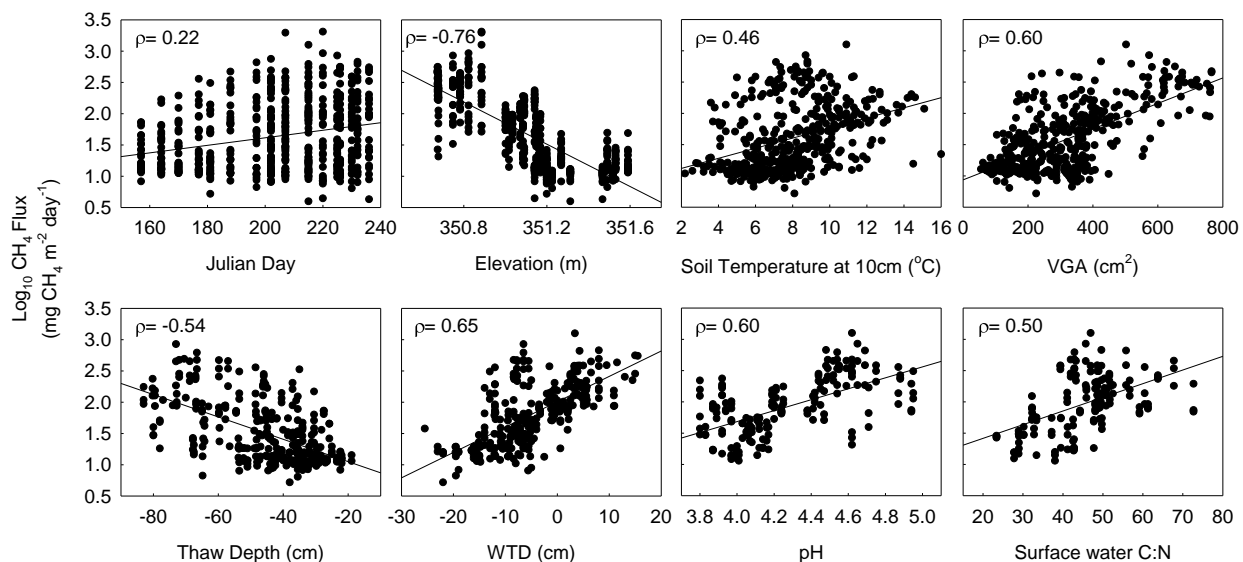
738  
 739  
 740  
 741  
 742  
 743  
 744  
 745  
 746  
 747  
 748  
 749  
 750  
 751

752 **Table 5.** Multiple regression model of CH<sub>4</sub>:CO<sub>2</sub> explained by percent cover of *Sphagnum* and  
753 soil temperature. ( $R^2=0.86$ ,  $F_{3,11} = 16.8$ ,  $p= 0.0008$ ). Estimates and standard errors (SE) are  
754 reported along with t-ratio and p-value.

	Estimate	SE	t-ratio	p-value
Intercept	2107.1	444.1	4.75	0.0015
Soil Temperature	-232.5	58.6	-3.97	0.0041
% <i>Sphagnum</i>	-3.0	0.5	-5.71	0.0004
Soil Temp x % <i>Sphagnum</i>	11.8	3.5	3.39	0.0095

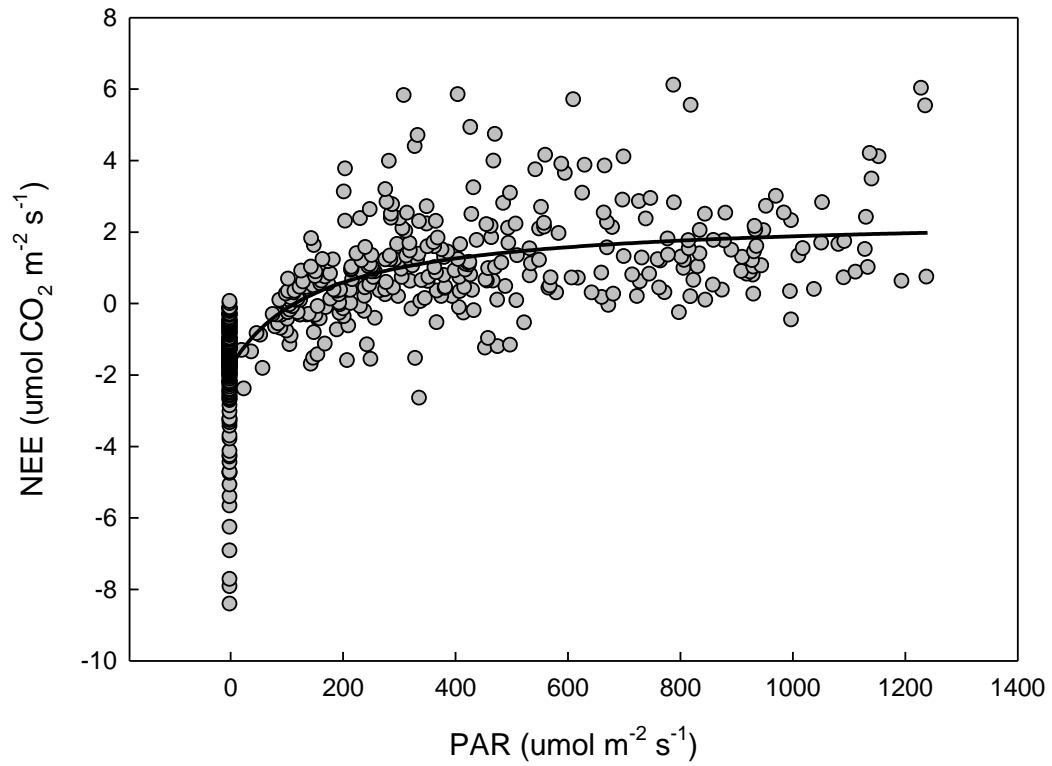
755  
756  
757  
758  
759  
760  
761  
762  
763  
764  
765  
766  
767  
768  
769  
770  
771  
772  
773

774 **7 Figures**



775  
 776 **Figure 1.** Relationship between the methane fluxes measured over two years and various  
 777 environmental variables (across peatland lumped data). Methane flux across 28 sampled collars  
 778 from two years (19 days of sampling) showed significant relationships with Julian day, elevation  
 779 (above sea level) of collar, soil temperature at 10 cm depth below surface(<sup>0</sup>C), modeled VGA  
 780 (vascular green area;cm<sup>2</sup>), water table depth (WTD), pH, thaw depth and C:N of surface water.  
 781 Spearman's  $\rho$  of each correlation are shown on each graph ( $p < 0.0001$ ).

782  
 783  
 784  
 785  
 786  
 787  
 788  
 789  
 790  
 791



792

793 **Figure 2.** Rectangular hyperbola fit of site-level NEE with PAR (n= 525).

794

795

796

797

798

799

800

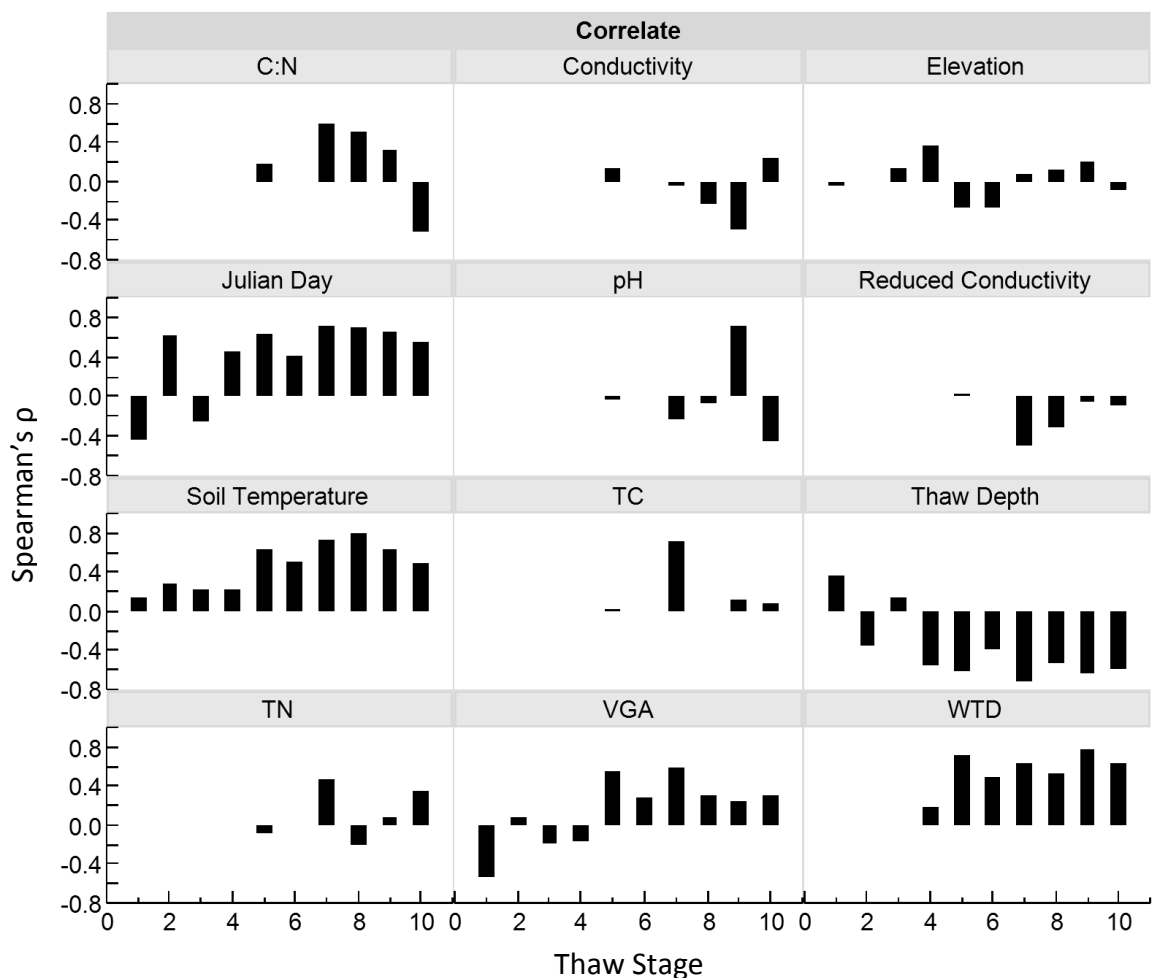
801

802

803

804

805



806

807

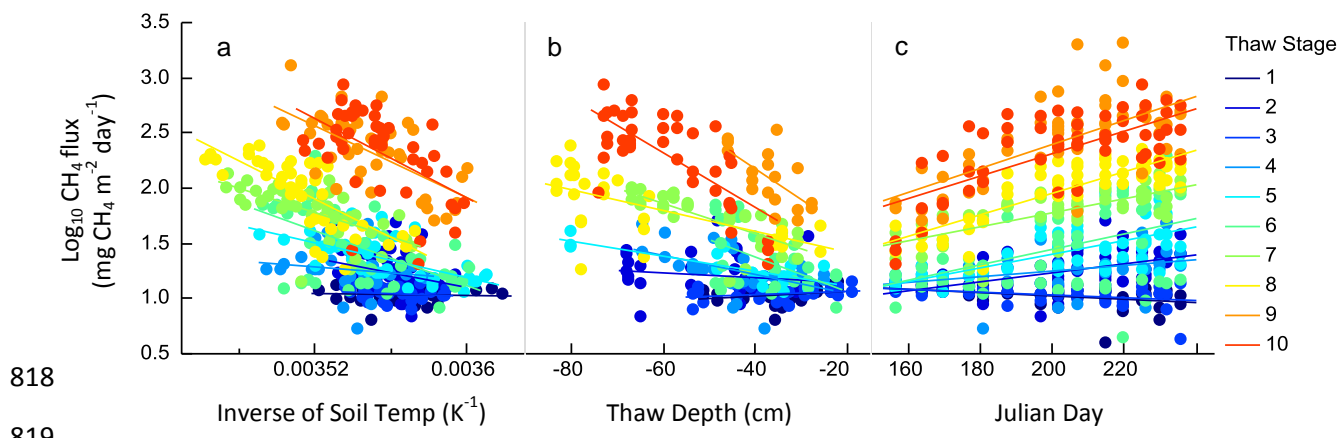
808 **Figure 3.** Correlation coefficients between CH<sub>4</sub> flux and various biotic and abiotic variables  
 809 along the thaw gradient from 1 to 10, where 1 is intact permafrost and 10 is fully thawed. Each  
 810 data point represents correlations analysis of n=19 days. The missing data points in WTD,  
 811 Conductivity, Reduced Conductivity, pH, TC, TN and C:N (total carbon, nitrogen and C:N in  
 812 surface water) are from the thaw stages that did not have a water table or had a correlation  
 813 coefficient of zero.

814

815

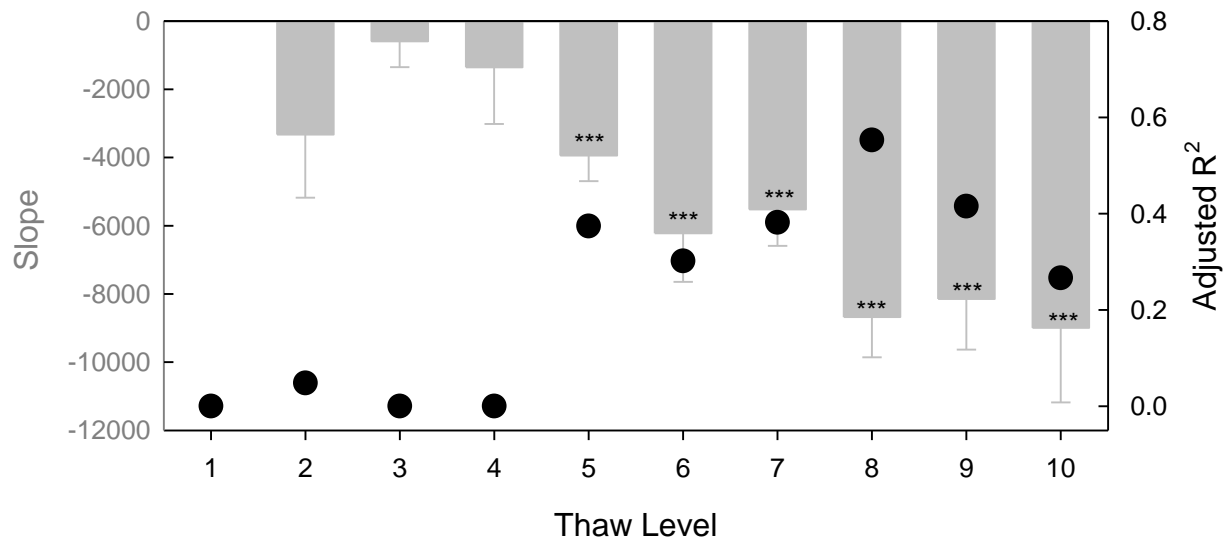
816

817



818  
819  
820  
821  
822  
823  
824  
825  
826  
827  
828  
829  
830  
831  
832  
833  
834  
835  
836  
837

**Figure 4 (a)** Arrhenius plots for each thaw stage. Slope and  $R^2$  of the plots increases with increased thaw (Figure 6). **(b)** changing linear fit between thaw depth and  $\text{CH}_4$  flux with progressing thaw. **(c)** increase in seasonality of  $\text{CH}_4$  flux as the permafrost thaws.



838

839 **Figure 5.** Slope and adjusted R<sup>2</sup> of the Arrhenius plot (Figure 4a) across the thaw stages. The left  
 840 y axis is the estimate and standard error of the slope of the fit (represented by the gray bars±SE)  
 841 and the right y axis shows the R<sup>2</sup> of each fit (represented by the black dots±SE). The significant  
 842 regressions (p<0.0001) are denoted by asterisk. Variance of methane fluxes explained by soil  
 843 temperature generally increases and becomes more significant (p-values) from less to more  
 844 thawed stages. Slope of the soil temperature to methane flux relationship also increases with  
 845 increased thaw.

846

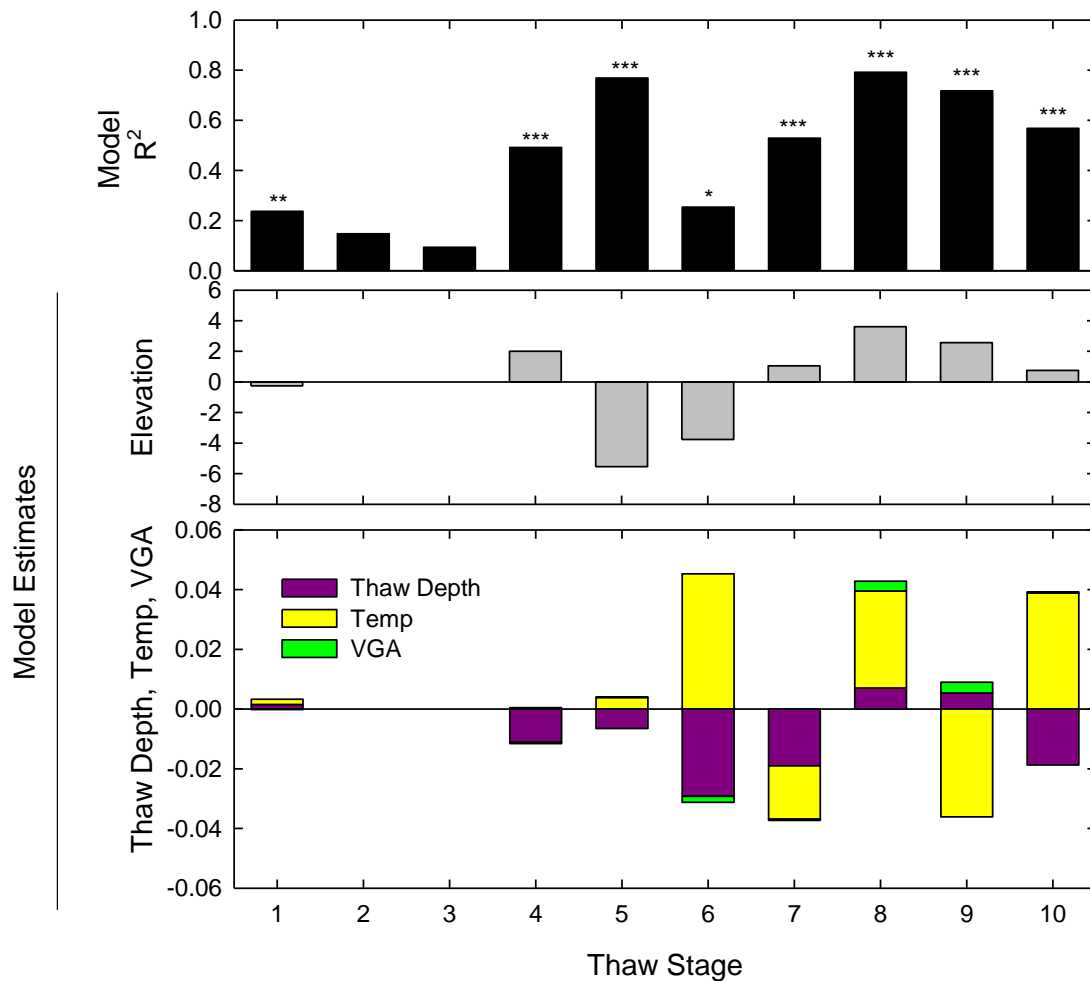
847

848

849

850

851



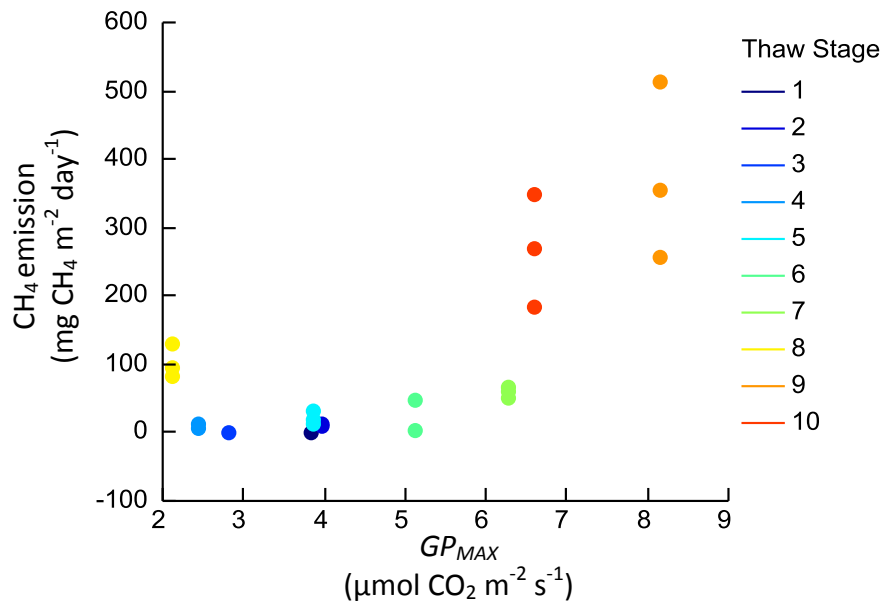
852

853 **Figure 6.** Multiple regression of CH<sub>4</sub> fluxes with elevation, thaw depth, soil temperature (Temp)  
 854 and vascular green area (VGA) for each thaw stage (Thaw stage 1= intact permafrost, 10=  
 855 completely thawed). Model fit R<sup>2</sup> values are reported along with model estimates (stacked bars).  
 856 Significance of the R<sup>2</sup> is denoted by asterisk (\* for p<.05, \*\* for p<.01, and \*\*\* for p<.001). Soil  
 857 Temperature was not a statistically significant estimate for any of the thaw stages. Elevation was  
 858 significant for thaw stages 1, 4, 8 and 9; thaw depth for 1, 4, 5, 7, 8 and 10; and VGA for 8 and  
 859 9.

860

861

862



863

864

865 **Figure 7.** Significant correlation between growing season means of CH<sub>4</sub> flux and GP<sub>MAX</sub> across  
 866 all thaw stages. Thaw stage 1 (intact permafrost) to 10(thawed permafrost) are shown using blue  
 867 to red colours.

868

869

870

871

872

873

874

875

876

877